REVIEW

An Invited Review for the Special 20th Anniversary Issue of MRMS

MR Imaging in the 21st Century: Technical Innovation over the First Two Decades

Hiroyuki Kabasawa[1*]

Clinical MRI systems have continually improved over the years since their introduction in the 1980s. In MRI technical development, the developments in each MRI system component, including data acquisition, image reconstruction, and hardware systems, have impacted the others. Progress in each component has induced new technology development opportunities in other components. New technologies outside of the MRI field, for example, computer science, data processing, and semiconductors, have been immediately incorporated into MRI development, which resulted in innovative applications. With high performance computing and MR technology innovations, MRI can now provide large volumes of functional and anatomical image datasets, which are important tools in various research fields. MRI systems are now combined with other modalities, such as positron emission tomography (PET) or therapeutic devices. These hybrid systems provide additional capabilities.

In this review, MRI advances in the last two decades will be considered. We will discuss the progress of MRI systems, the enabling technology, established applications, current trends, and the future outlook.

Keywords: *magnetic resonance imaging, magnetic resonance imaging system, image acquisition, image reconstruction, magnetic resonance imaging applications*

Introduction

MRI was introduced in the early 1980s as a clinical diagnostic device. Since then, there has been a lot of technological development. In MRI technical development, advances in each MRI technical component, including data acquisition, image reconstruction and hardware systems, have interacted with each other. Progress in each component has induced new technological development opportunities in other components. New technologies in basic sciences and engineering, for example, computer science, data processing, and semiconductors, have been immediately incorporated into MRI development, which results in innovative applications (Fig. 1).

[1]Department of Radiological Sciences, School of Health Sciences at Narita, International University of Health and Welfare, Narita, Chiba, Japan

*Corresponding author: Department of Radiological Sciences, School of Health Sciences at Narita, International University of Health and Welfare, 4-3, Kozunomori, Narita, Chiba 286-8686, Japan. Phone: +81-476-20-7701, Fax: +81-476-20-7702, Email: kabasawa@iuhw.ac.jp

Magnetic Resonance in Medicine is a unique medical research field based on Magnetic Resonance Imaging and Spectroscopy (MRI/S) technology. MRI/S technology is the core part of this research field, and the advance of the technology leads to further success in MR medical research. The various needs of clinical radiologists and basic medical research scientists have always been invaluable inputs for technology innovation, stimulating MR technical development and resulting in new imaging technologies. The medical research community utilizes new imaging technology to achieve innovative clinical results. Collaboration between diverse people in the MR community is the key to the success of technical development and research. To celebrate the 20-year anniversary of the Magnetic Resonance in Medical Science (MRMS) journal, MR technology development, progress, and its application to clinical research in the last 20 years will be reviewed and discussed. In this short review, MR technology progress will be covered, starting with MR systems technology, followed by application development, including pulse sequences, image reconstruction, and data analysis.

MR System Development

The 1.5T clinical MRI was launched as a commercially available clinical system in the early 1980s. The key MR system
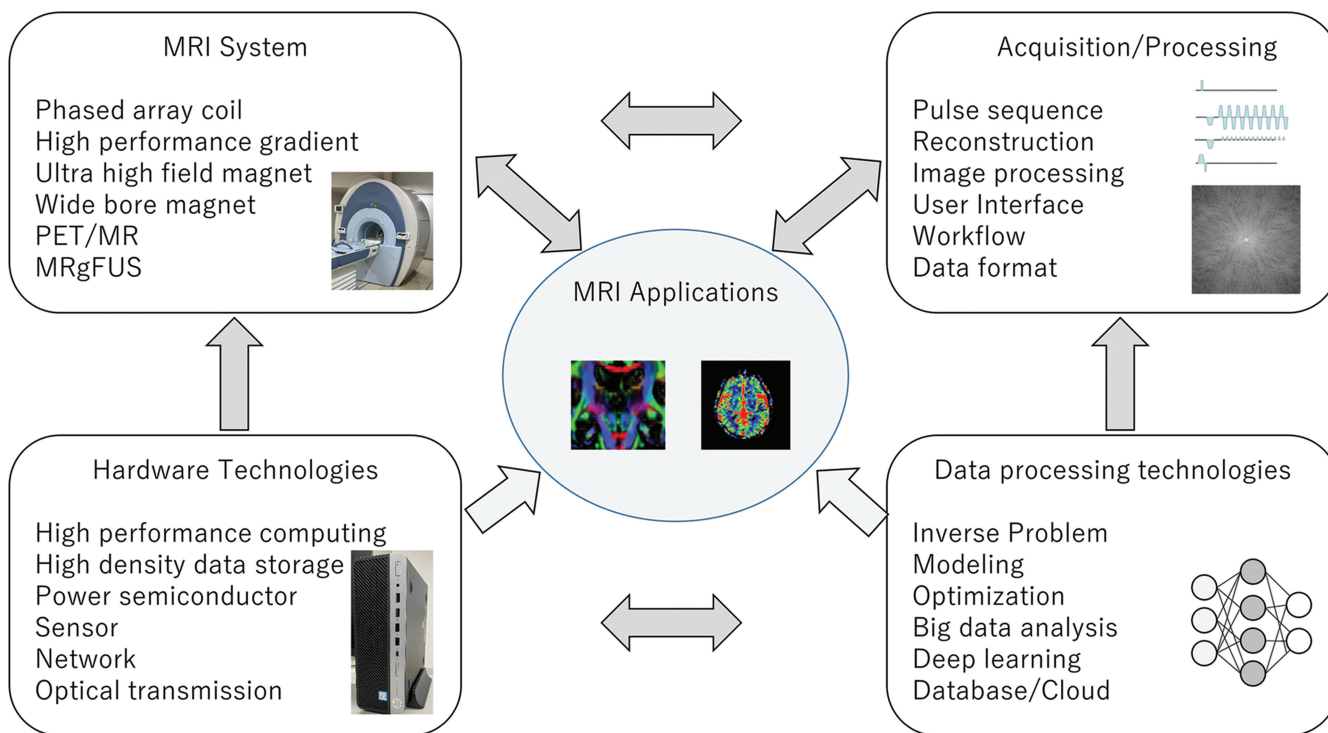
Fig. 1 MRI technology advances and the interactions between each technical component. Technical advances in basic sciences and engineering impact MRI technologies. Technical development needs in each element drive innovation in other elements. MRgFUS, MR-guided focused ultrasound; PET, positron emission tomography.

technologies, such as superconductive high-field magnet, shielded gradient coil, phased array coil, and so on, were developed in the first 20 years. Despite the fact that key elements of MRI had been established by the year 2000, technology advances in the last two decades are still worth consideration. A lot of significant achievements have been made and it would be difficult to mention them all; however, ultra-high-field MRI, high-density phased array coil, and hybrid MRI systems are among the most significant innovations. Both ultra-high field and coil density contributed to high SNR, resulting in improved image quality and advanced applications.

The clinical 3T system was regulatory approved and introduced in the early 2000s. At that time, the anticipated 3T clinical applications were higher spatial resolution imaging and faster imaging.[1–3] The 3T whole body system was then developed and made commercially available.[4,5] It spread rapidly throughout the later 2000s. A major technical innovation for the clinical 3T MRI system was magnet technology with reasonable cost and the RF transmit, and receive system. In addition, specific absorption rate (SAR) management application technology was another key improvement to make it available as a reasonable clinical MRI.

Nowadays, most academic centers have a 3T MRI system, and it is the main platform for both clinical practice and MR research/technical development. 3T clinical system development focuses on two different directions: One is pursuing higher system performance to achieve better image quality, and the other is prioritizing patient comfort, such as by using a wide bore MRI system while maintaining clinically acceptable performance.

For MRI systems higher than 3T, major MRI manufacturers started to develop a human 7T system from the early 2000s that was in operation by the mid-2000s. Now, at the end of 2020, some MRI manufacturers have received regulatory approval for their 7T systems. The advantage of a 7T system is higher SNR that correlates with field strength; therefore, high spatial resolution imaging[6] is one of the potential applications for 7T (Fig. 2).

As human scan experience has been accumulated at 7T research sites, safety investigation reports have been published. It has been reported that vertigo and feelings of curving during table movement were the most frequent sensations during 7T scanning. Rapid field change could cause these transient sensations, and it may be possible to reduce their occurrence with slower table speed and careful subject handling.[7]

RF penetration and uniformity has been a major challenge for high-field MRI,[8] particularly at 7T or higher. In high static magnetic field, dielectric resonance associated with shorter RF wavelength and penetration depth results in destructive wave interference that causes transmit RF field uniformity. RF transmission technologies, such as RF shimming and parallel transmit (pTx), can optimize RF uniformity using B_1/B_0 field measurement data. Obviously, B_1/B_0 field measurement quality directly impacts the RF uniformity optimization result. In the ultra-high field, it has been reported that subject
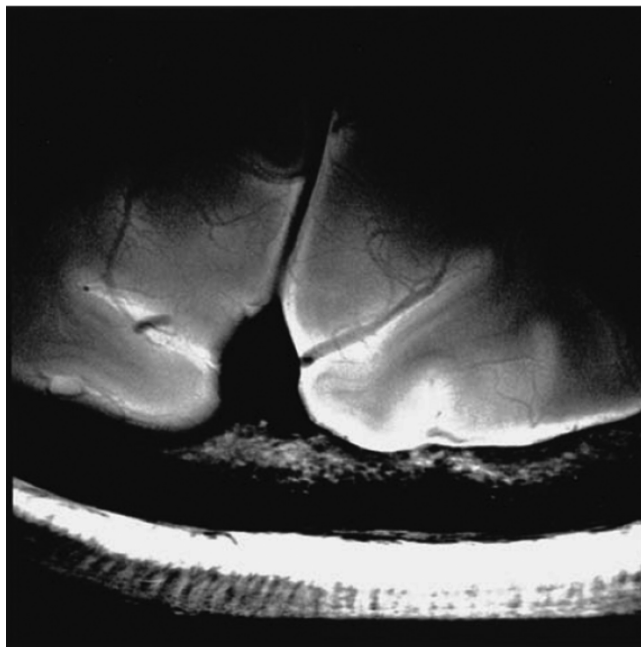
Fig. 2 An example of a high resolution 7T Brain image (adapted from Fig. 6 of Nakada et al.[6]). The image was obtained with an FSE sequence with peripheral gating utilizing a single receiver channel of an 8-channel receiver coil. The main parameters were as follows: TR = 6 cardiac cycle, TE = 30.264 ms, trigger delay = 500 ms, FOV = 5 x 5 cm, matrix size = 512 x 512, NEX = 2, and echo train = eight. NEX, numbers of excitations.

respiratory motion could cause B_0 field fluctuation;[9] however, its impact on pTx image quality is not fully understood. Breath-holding B_1 mapping acquisition could help reduce pTx image quality variation.[10] Improved acquisition ordering has provided reduced sensitivity to subject motion in pTx imaging.[11] These key findings are important for human pTx scans and make the scan robust in real-life conditions.

Phased array coil was invented in 1990.[12] It has been implemented and available on clinical scanners since then. The role of the phase array coil became more important when parallel imaging (PI) technology was introduced on clinical MRI in the early 2000s.

Advancement in information and communication technology, including fiber-optic communication systems, RF relevant semiconductors, and digitizers, has led to RF transmit and receive (Tx/Rx) chain hardware improvement. The MRI analog transceiver was replaced by a digital one, and the MR signal is now digitized in the MR room and transferred through optical fiber to the system. Both changes have contributed to significant SNR improvement. Technology improvement in RF consumer semiconductor products resulted in an increasing number of RF channels with a small foot-print and low cost. The number of receive coil channels, or as we call it, coil density, has increased continually over the last two decades.[13] Clinical MRI systems now have the capability to connect to more than 100 RF coils. High-density phased array coils with 32 or 64 receive channels can be used on clinical systems that have better imaging speed capability with PI.

Minimizing interaction between coils is critical to optimizing phased array coil performance. This mutual coil coupling restricted phased array coil design, such as fixed geometry, coil size limitation, and limited sensitivity penetration.[14] Recently, a high impedance flexible coil element that can be used to design wearable MR receive coils has been proposed. This innovative technology provides improved SNR, higher g-factor, and improved patient comfort. Such an RF technology combined with advanced PI is a key innovation for scan speed acceleration across all body areas.

Advancements in power semiconductor devices, such as insulated gate bipolar transistors (IGBT) and power metal-oxide-semiconductor field-effect transistors (power MOSFET), have driven improvements in MR gradient and RF amplifier hardware. These semiconductor devices enable us to control gradient and RF waveform with better fidelity. They also contribute to providing higher performance in terms of gradient and RF. In addition, they help reduce the energy consumption, cost, and foot-print of the MRI system.

With advances in semiconductor photon detection devices, integrated PET-MRI has been developed and implemented as a clinical scanner.[15] The MR-specific research area is relatively limited; however, interesting studies have been conducted, including pseudo-CT image synthesis from MR images for attenuation correction,[16,17] lung imaging with zero TE,[18] arterial spin labeling cross-validation,[19] and whole-body diffusion cross-validation with PET imaging. On the other hand, a PET detector insert combined with MRI transmit and receive coil system has been developed.[20] As we have a large MR install base, there will be an opportunity to use a similar PET detector at existing MRI sites, and that will lead to an improved access to PET/MRI system.

Therapeutic intervention in the bore is one of the important MRI system innovations over the last two decades. The MR-guided focused ultrasound (MRgFUS) system was introduced for uterine fibroids treatment,[21] and then its application for essential tremor treatment[22] was developed. MRI is used for the treatment planning and temperature monitoring in the MRgFUS intervention. Tissue temperature change during the MRgFUS treatment is monitored to control energy delivery from an ultrasound transducer. The temperature change can be monitored non-invasively using MR signal phase change.[23]

Image Acquisition

As discussed in the previous section, the performance of MRI system hardware components, including gradient slew rate, maximum gradient strength, RF power, and number of RF channels, has been significantly improved. Image data acquisition technology continues developing with these hardware improvements. In 1990, fast spin echo (FSE), echo planar imaging (EPI), and fast gradient echo sequences were developed. These sequences rely on gradient and RF hardware performance. The image quality of these sequences improved as MRI hardware performance improved. For these methods, faster k-space filling, for example, shorter echo spacing or shorter TR provides better image quality.

In the last two decades, a k-space data sampling strategy and reconstruction started to be used as another fast imaging technology approach. Basic PI concepts, such as simultaneous acquisition of spatial harmonics (SMASH)[24] and sensitivity encoding (SENSE),[25] were proposed at the end of the 1990s. Subsequently, a variety of improved PI methods have been proposed based on these two original technologies.[26–29] PI had been implemented in clinical scanners by the mid-2000s, and then became a standard image acquisition method used in routine clinical practice. The advantage of PI compared with other fast imaging is that it basically maintains image contrast and is compatible with most image acquisition sequences. A disadvantage of PI is SNR reduction associated with k-space sampling reduction and RF coil geometry. As the density of phased array coil has continued increasing throughout the decades, PI acceleration factor has also kept increasing. A factor of two was commonly used for clinical scans at first. Then, a factor of 4 or more could be used for 3D acquisition with 2D PI. Scan time can be further reduced in combination with partial Fourier imaging[30,31] (PFI) and compressed sensing[32,33] (CS). CS is a relatively new (proposed in 2007) iterative image reconstruction method. It uses image sparsity to reconstruct an MR image with under-sampled k-space below the Nyquist frequency sampling limit. Because CS only uses image information characteristics for image reconstruction, this iterative method can be combined with PI and PFI simultaneously. A lot of studies are being conducted on how to optimize k-space sampling reduction, how to reconstruct the acquired data, and how to combine these three reconstruction methods. These combined methods provide scan time reduction of around 10 times, even on commercial MRI scanners.

The fast imaging method with PI provides a long list of benefits in clinical MR imaging, particularly in the body and cardiac area, as these organs keep moving along with the cardiac and respiratory cycles, thus shorter scan time directly links to high image quality.[34] With most recent advanced PI methods, even high special resolution 3D imaging can be completed within a breath-hold period.[35]

If organ motion is periodical, similar motion is repeated over the cardiac and respiratory cycle. Thus, information redundancy exists in the MRI data, which can provide a further data sampling reduction opportunity in the time domain. Sampling reduction in t-space is generally combined with k-space reduction, and then acquired k-t space is reconstructed by a dedicated method.[36] This data sampling reduction in the k-t space provides high performance in cardiovascular imaging.[37] Phase contrast 3D cine imaging, so-called 4D flow, requires 7-dimensional data, including 3D spatial, cardiac cycle, and 3D flow encoding, which is difficult to acquire within clinically available scan slots. The k-t acceleration helps us make the 4D flow available in clinical settings; thus, the k-t method is a big break-through technology for vascular imaging.[38]

2D single-shot EPI imaging samples a whole k-space data in single RF excitation and it is thought to be sufficiently fast enough; however, its acquisition speed is still limited by hardware performance and safety limits. There were growing needs for scan time acceleration for quantitative parametric imaging in neuroscience. Simultaneous multi-slice (SMS) imaging is a method to acquire multiple slices in a single RF excitation. This acquisition method enables us to increase the number of slices in a given TR, thus MRI scan time is decreased. Simultaneous multi-slice excitation was originally proposed in the early 1990s.[39] The original method used different RF phase modulation for each excitation with multiple numbers of excitations (NEX) so as to separate slices by Fourier transform. A novel SMS method based on RF coil sensitivity information and gradient phase encoding was developed, which could be used with a single-shot acquisition sequence.[40] This advanced acquisition and reconstruction technology is now an essential tool for MR neuroscience research. In addition, it has been used for scan time reduction for clinical diffusion MRI scans.

Motion Robust Imaging

An MRI scan generally consists of multiple RF excitations and data acquisitions. Multiple-shot acquisition is sensitive to the subject's motion because the motion may cause additional modulation in the image data for each shot. Each shot may include different motion-induced phase shift in the MR signal that results in ghosting. From the early days of MR imaging technology development, motion-induced ghost reduction methods have been developed and used. The methods include motion synchronized acquisition and sorted k-space data acquisition ordering to put the artifact out of the FOV.
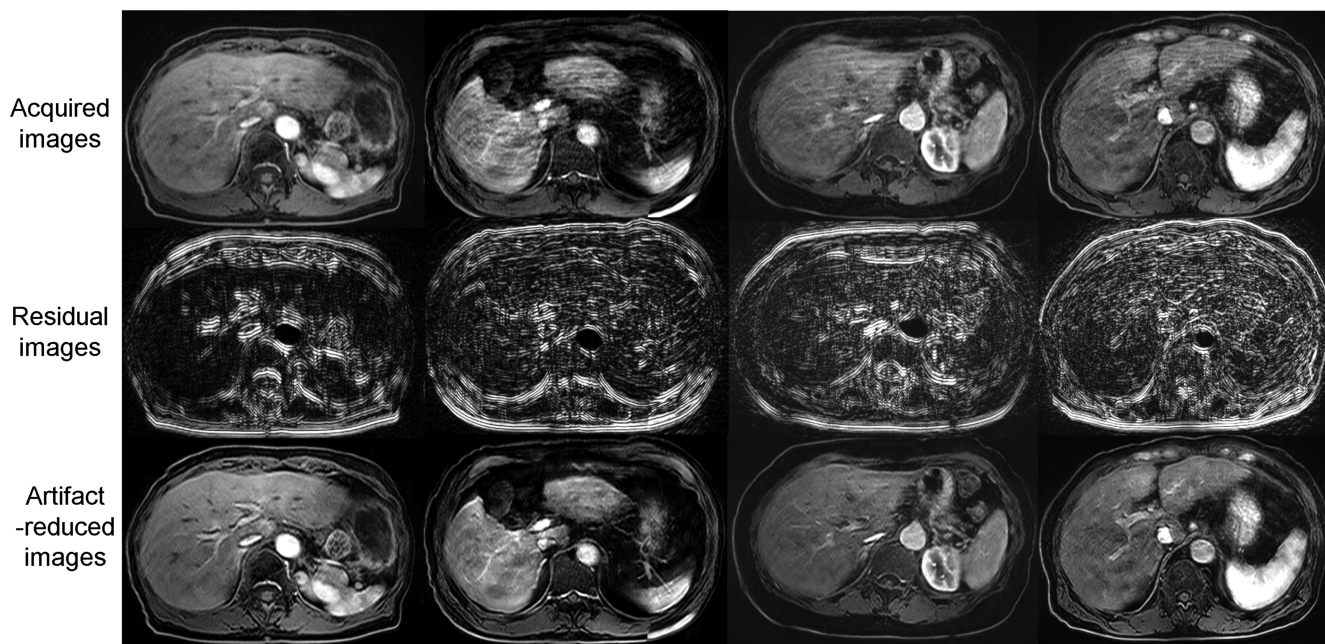
Fig. 3 Examples of deep learning-based motion artifact reduction. The motion artifacts in the acquired images (upper row) were reduced (lower row). The residual components are shown in the middle row (adapted from Fig. 10 of Tamada et al.[50]).

External devices, such as bellows, have been used to monitor motion. Later, navigator pulse sequences, which consist of 1D or 2D spatial selective excitations and projection data readouts with TR of 20–100 ms, have been used to monitor the subject's motion. The navigator pulse can measure organ location directly, whereas an external device detects body surface motion. Thus, better motion correction performance is anticipated with a navigator. Previously, navigators have been used for motion triggered scans, but they can now be used for gated scans. With this gated navigator acquisition, abdominal 3D acquisition was freed from the breath-hold time limit. As a result, this technique provides excellent T1 3D high-resolution abdominal imaging with a scan time longer than breath-holding.[41]

On the other hand, retrospective motion correction without using an extra monitor signal has been developed to improve MRI motion robustness. For 2D imaging, radial k-space trajectory with a self-navigator has been used for motion robust acquisition.[42] Periodically rotated overlapping parallel lines with enhanced reconstruction (PROPELLER)[43] acquires concentric rectangular strips which consist of a few k-space lines. As it has 2D image information within each shot of acquisition, it has image-based motion detection and a correction algorithm incorporated in it.

For 3D imaging, the radial stack of star (SOS) k-space trajectory has been applied to de-sensitize MR imaging from motion effect. Because the SOS samples k-space data radially in the kx-ky plane and sequentially in the kz-direction, it has a zero-frequency k-space center signal in every kz loop. Hence, it has motion-monitoring capability. The kx-ky pseudo-random radial sampling order was implemented with golden angle acquisition, and the motion effect on the MR image can be seen as a random incoherent ghost in various directions. The monitored subject's motion can be used to reduce the motion effect. This method has been used for 3D contrast-enhanced dynamic abdominal imaging. As it is motion insensitive, it can provide free-breathing high temporal resolution 3D CE-dynamic imaging.[44,45]

Another 3D motion insensitive approach is pseudo-random 3D k-space filling in the ky-kz standard Cartesian acquisition. In this way, pseudo-random k-space trajectory scanning effectively suppresses motion artifacts in T1-weighted images.[46]

For brain 3D imaging, prospective rigid motion correction using a 3D navigator has been developed[47] and used. Head motion is monitored with 3D navigator acquisition and the measured information is used to collect acquisition location, which provides a prospective correction capability. It has been reported that the method is useful for brain volume measurement.[48]

Recently, new motion detection technologies have been developed and become available for MRI motion correction. These devices perform the subject's motion detection from a camera,[49] detecting coil load signal change by motion and B_0 field change monitoring. These advancements are expected to provide better motion robust acquisition technology.

Image Reconstruction

Computational power has continued to increase in the last two decades. As computer performance has improved, the volume
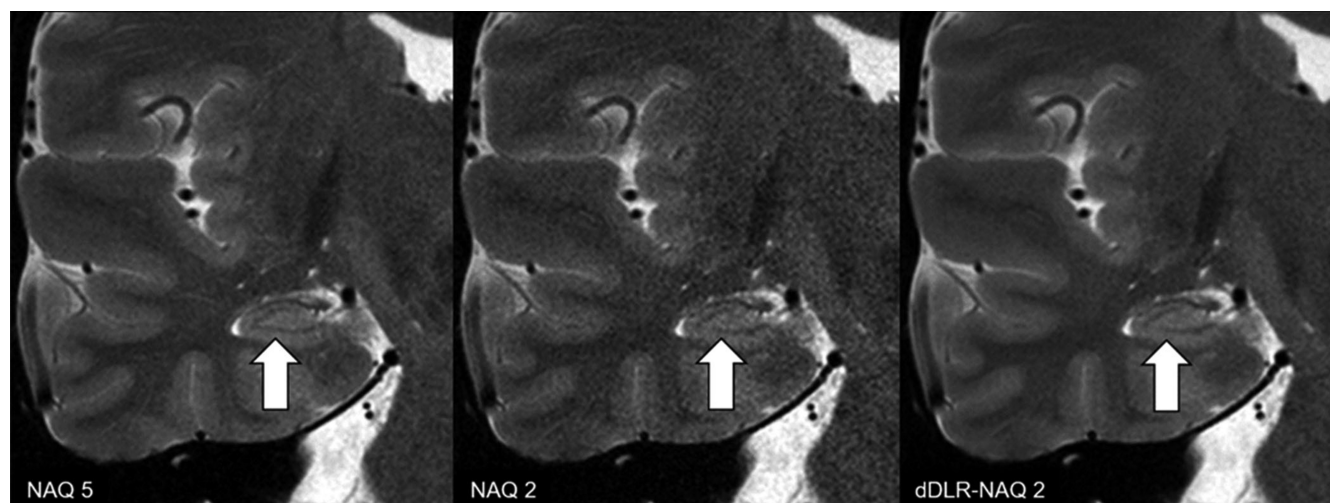
Fig. 4 T2-weighted image reconstructed by dDLR. NAQ2 has higher image noise than NAQ5 and dDLR-NAQ2. Identification of the hippocampal layer structure is superior in both NAQ5 and dDLR-NAQ2 compared with NAQ2 (arrows) (adapted from Fig. 7 of Kidoh et al.[51]). dDLR, deep learning-based reconstruction; NAQ, number of image acquisition.

of MRI data that we can process within a given time has continued to increase. Thanks to the technical innovations in MRI hardware and data acquisition technology, the number of data points that MRI can produce has been increased to the level of gigabytes in one acquisition. MRI data are now large dimensional data in the spatial, temporal, coil channel, and parametric domains (flow, diffusion). For example, diffusion tensor acquisition may have high-dimensional data, including 100 slices, 32 channel coils, and 100 diffusion encodings, which results in 320000 slices. 4D flow data may include 100 slices, 32 channel coils, and 4 flow encodings with 24 cardiac phases, which also results in 300000 slices.

The latest advanced image reconstruction involves a large number of calculations, including PI, compressed sensing, phased array coil combinations, and so on. State-of-the-art clinical MRI scanners need to reconstruct such high-volume 3D MRI data within examination time or a reasonable wait time after complete examination.

Artificial intelligence (AI) technology, particularly deep learning (DL) algorithms, has accelerated innovation in MR image reconstruction. Motion artifact reduction and motion robust image reconstruction are some of the areas where DL can provide significant improvement. A subject's motion is not generally predictable; thus, deterministic algorithms are not effective for motion correction. As illustrated in Fig. 3, DL algorithms have successfully reduced the motion artifact from 3D contrast-enhanced dynamic T1-weighted liver images with a numerically generated artifact image learning method.[50]

SNR improvement can be achieved with DL algorithms. High SNR images with many excitations and low SNR images with few excitations were prepared and put into the learning algorithm. The generated neural network could provide high SNR images from low SNR ones[51] (Fig. 4). Until now, MRI SNR has had a trade-off relationship with scan time and spatial

resolution. As a result, some scan parameters could be compromised to balance image quality and scan time. New DL denoising reconstruction allows us to use scan protocols previously unavailable due to low SNR. It has already been applied to thin slice acquisition with shorter scan time, high spatial resolution 3D volume image acquisition, and so on. It has been reported that DL denoising can provide 3T equivalent image quality from 1.5T images.[52,53]

Workflow

Automation and workflow improvement play critical roles in reducing non-value-added time[54] during MR examination. Scan plan selection and location flexibility are advantages of MRI. However, these advantages can lead to challenges for scan operators when they prescribe scan plans for complex anatomy scans. These challenges constitute drawbacks of MRI examination, such as operator-dependent prescription, long examination time, and scan availability when experienced scan operator availability is limited. The latest sophisticated software may be able to provide a similar performance as an experienced expert operator. Image feature detection and knowledge-based algorithms can recognize cardiac anatomy and prescribe scan locations automatically[55] (Fig.5). The algorithms can be further improved, expanding the application to many body areas using DL methods.[56] Other than cardiac slice prescription, many workflow improvement efforts have been made, for example, brain automated slice prescription,[57] liver automated slice prescription,[58] and bolus tracking region of interest.[59]

The introduction of the Digital Imaging and Communications in Medicine (DICOM) image format was a baseline of image-related workflow innovation in this decade. This common image format allows us to
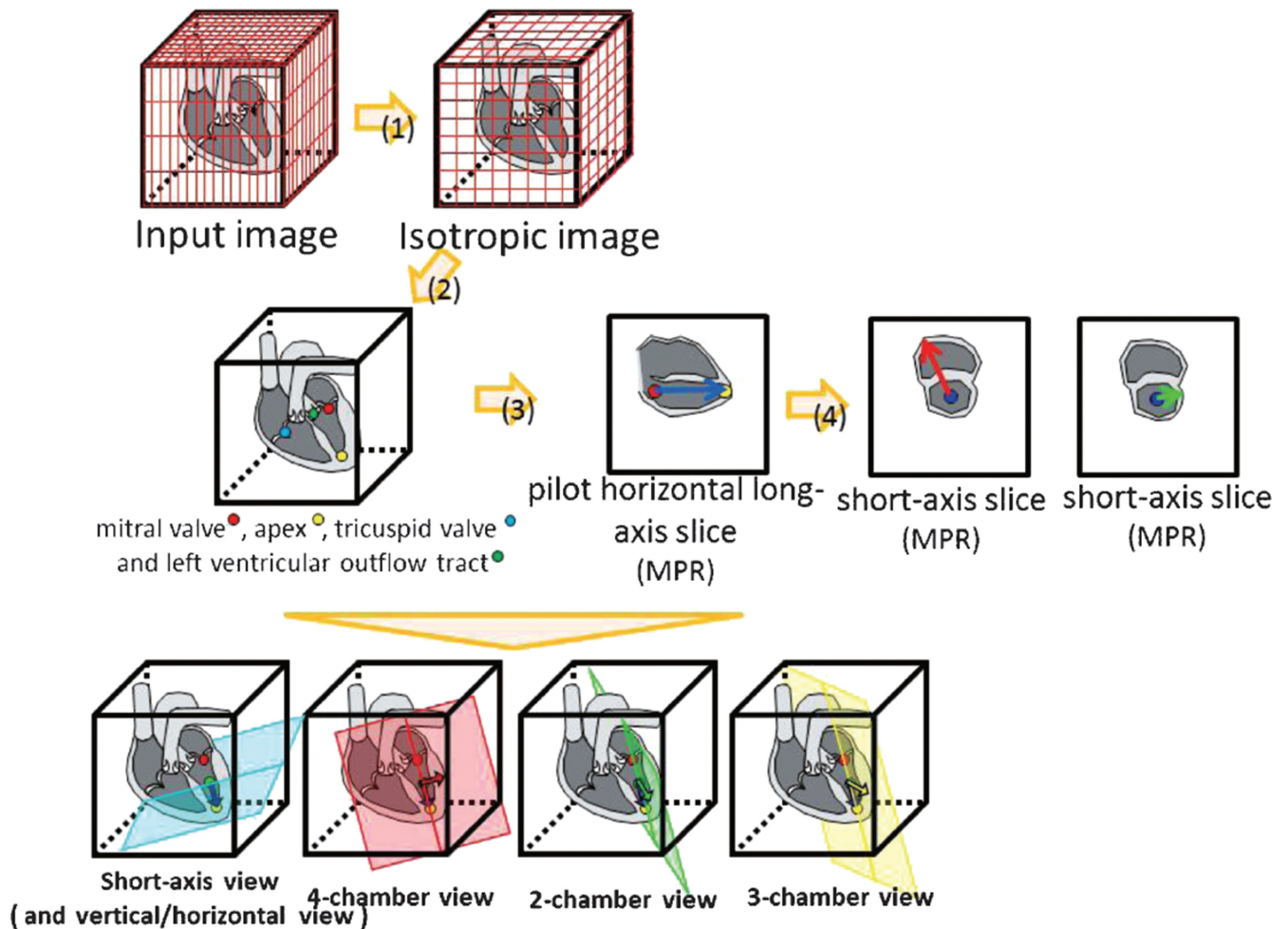
Fig. 5 An automated cardiac slice prescription process flow. Mitral valve, apex, tricuspid valve, and left ventricular outflow tract were detected. These reference points were used to prescribe scan slices such as short-axis view, 4-chamber view, 2-chamber view, and 3-chamber view (adapted from Fig. 1 of Yokoyama et al.[55]).

transfer, view, and process MR images without any significant technical skill. It has resolved all the workflow issues related to image data. It has significantly improved the access to MR image data, which results in image processing analysis innovation, particularly quantitative and functional image analysis.

Vascular Imaging

Non-contrast MR Angiography (NCE-MRA) has been a key topic for pulse sequence development in the last two decades. Labeling technology has been the core technology to obtain high-quality angiogram, while fast imaging is another key element of the imaging method to obtain abdominal MRA. Fresh blood imaging (FBI)[60] was an innovative labeling method that used blood flow speed difference between diastolic and systolic phases. The inversion-based labeling method has been used in clinical abdominal non-contrast MRA imaging.

Most non-contrast vascular imaging sequences are based on FSE or a steady state in free precession (SSFP) sequence, with which the blood signal is visualized as high signal on the image.[61] Respiratory triggered scan is frequently used for body MRA acquisition due to its long scan time. Moreover, the combination of compressed sensing and PI reduced scan time that led to breath-hold abdominal non-contrast 3D MRA imaging.

Head-neck MRA is the remaining area for NCE-MRA technological development, as B_0 and B_1 uniformity degrade the image quality. Improved FSE-based NCE-MRA has shown promising results in the neck region.[62] Peripheral NCE-MRA is another challenging area because of B_0 and B_1 uniformity and slow flow speed. A flow acceleration encoding MRA method has successfully improved reproducibility of MRA in peripheral areas.[63]

A combination of spin labeling and the advanced reconstruction method results in time-resolved NCE-MRA, which provides flow information with high temporal resolution on

the MRI. This technology further combined with arterial spin labeling (ASL) perfusion imaging can generate MR angiography and perfusion imaging in a single acquisition.[64]

Recent vascular treatment involves metal implant devices, such as an aneurysm coil or stent. MRA acquisition was sensitive to these metal implants; however, ultrashort TE or zero TE MRA can provide excellent MRA with reduced susceptibility to these devices.[65] This advanced acquisition was enabled by high RF and data sampling switching hardware. Invasive follow-up examination with interventional angiography can be reduced with this advanced MRA sequence.

Image Contrast and Quantitative Imaging

Diffusion MRI (dMRI) came into use on clinical MR scanners in the mid-1990s. Since then, technology has been significantly improved to provide many advanced applications, including intravoxel incoherent motion (IVIM),[66] diffusion tensor imaging (DTI) and DTI-based tractography,[67] diffusion kurtosis imaging (DKI),[68] etc. These dMRI methods have been necessary tools for neuroscience research to understand brain microstructure and connectivity.[69] Single-shot EPI has been used for dMRI acquisition sequences, which limits spatial resolution and image quality. While various high spatial resolution dMRI acquisition pulse sequences have been proposedand used[70–72] in the last decades, there are remaining improvement opportunities to balance scan time, image quality, and spatial resolution.

Although chemical exchange has been a major research target in the in-vitro nuclear magnetic resonance (NMR) field for years, it has not been used in clinical MRI due to demanding hardware requirements. Chemical exchange saturation transfer (CEST) has been proposed to use chemical exchange as an image contrast. Continuous RF irradiation is required to saturate a molecule that has a certain resonance frequency. Saturation is transferred through a chemical exchange process, so that the exchange can be visualized as image contrast. CEST contrast is sensitive to micro-environmental properties of molecules.[73,74] It has been used to diagnose brain tumor. The hardware requirements for continuous RF irradiation are far different from standard clinical MR scanning. RF amplifiers for clinical MRI are generally designed to generate high peak power within a short period for fast imaging acquisition. Some MR manufacturers have already implemented the capability.

MR elastography (MRE) can provide image contrast associated with tissue elasticity. An elastic wave is generated by an external transducer, and the wave is sent to the body. MRI is used to visualize the wave field at multiple time points. The acquired wave field is reconstructed into the elasticity spatial distribution of the human body. It has been applied for liver cirrhosis diagnosis,[75,76] and then its application is expanded to measure brain tumor stiffness.

Magnetic susceptibility is a property of a material that reflects the reaction of the material to a magnetic field. Quantitative susceptibility mapping (QSM) is a way to measure magnetic susceptibility using MRI. Magnetic susceptibility changes the local magnetic field that induces local magnetic resonance frequency change. Local phase shift on an MR image can provide local magnetic field information. Inversion algorithms are used to estimate magnetic susceptibility spatial distribution from magnetic field measurement results. It is a non-linear ill-posed inverse problem, and many reconstruction methods have been proposed (Fig.6)[77,78] to solve it, including DL algorithms. Broad QSM applications have been studied, including oxygen extraction fraction mapping and carotid plaque imaging.[79]

Longitudinal relaxation time and transverse relaxation time (T_1 and T_2) have been studied as measurable quantitative parameters since the early days of MRI development. With recent advances in pulse sequence development, these traditional MR parameters can be acquired more quickly than ever before. Fast multi-parametric mapping methods, such as synthetic MR and MR fingerprinting, provide easier access to quantitative measurements.[80,81]

Future Outlook

There are a lot of topics that cannot be mentioned in this article as MR technology is too broad to be comprehensively covered. New contrast mechanism developments, including hyperpolarized MRI, and new contrast materials may bring us new imaging methods to see tissue metabolism and function.

As we have seen in the last several decades, advances in computing power have significantly impacted MRI innovation. As cloud services improve, all the intensive computer processing related to MRI, like large data handling and high performance computation, may be integrated into the cloud.[82,83] This will change the paradigm of MRI data flows. Mouses and keyboards have been the standard user interface (UI) for the last two decades. New UIs, such as smartphones, may introduce new interactions with MRI scanners and facilitate new MRI application development.

Sensing device technology and big data processing can provide better MR scanners and subject monitoring tools. These measurement results can be used as feedback information, which can help improve MR scan fidelity. Consequently, the performance of MR scanners will increase or similar performance can be achieved at lower cost.[84,85]

Challenges in healthcare economics and aging societies will bring about opportunities for new technology development. Low helium consumption and low-cost magnet would be a solution for sustainable MRI in challenging healthcare economies. Patient-centered technology development, such as wide bore systems, low acoustic noise scanning,[86,87] lightweight coil, and free-breathing scanning, will continue to be an important goal.

Finally, the importance of collaboration between MR manufacturers, physicists, radiologists, and technologists should
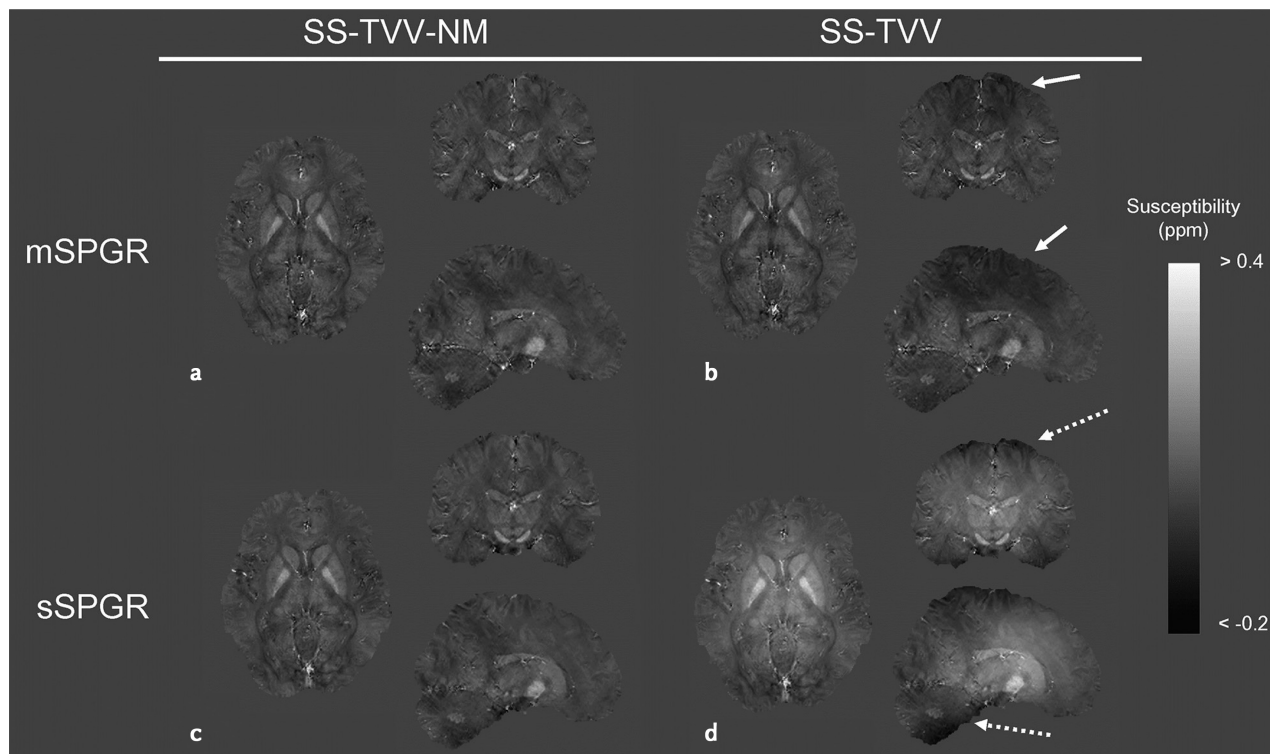
Fig. 6 Susceptibility maps estimated by SS-TVV-NM and SS-TVV from mSPGR and sSPGR, respectively. A slight signal inhomogeneity was observed in the map estimated by SS-TVV from mSPGR (dashed arrows). Moreover, a large shading was observed by the combination of SS-TVV and sSPGR (dashed arrows). mSPGR, multiple spoiled gradient echo sequence; sSPGR, single-echo spoiled gradient echo sequence; SS-TVV-NM, single-step total variation with variable kernel size and norm minimization within the volume of interest (adapted from Fig. 4 of Kan et al.[78]).

be emphasized. This collaboration is key to implementing new MRI advanced technology in clinical practice. It is the best source of innovation for MRI success in the future.

Conflicts of Interest

The author was an employee of GE Healthcare from April 1st, 1993 to March 31st, 2020. Most of the technical developments described in this review occurred during that period.

References

1. Fukatsu H. 3T MR for clinical use: update. Magn Reson Med Sci 2003; 2:37–45.
2. Sasaki M, Inoue T, Tohyama K, et al. High-field MRI of the central nervous system: current approaches to clinical and microscopic imaging. Magn Reson Med Sci 2003; 2:133–139.
3. Naganawa S, Kawai H, Fukatsu H, et al. High-speed imaging at 3 Tesla: a technical and clinical review with an emphasis on whole-brain 3D imaging. Magn Reson Med Sci 2004; 3:177–187.
4. Uematsu H, Takahashi M, Dougherty L, et al. High field body MR imaging: preliminary experiences. Clin Imaging 2004; 28:159–162.
5. Kataoka M, Kido A, Koyama T, et al. MRI of the female pelvis at 3T compared to 1.5T: evaluation on high-resolution T2-weighted and HASTE images. J Magn Reson Imaging 2007; 25:527–534.
6. Nakada T, Nabetani A, Kabasawa H, et al. The passage to human MR microscopy: a progress report from Niigata on April 2005. Magn Reson Med Sci 2005; 4:83–87.
7. Uwano I, Metoki T, Sendai F, et al. Assessment of sensations experienced by subjects during MR imaging examination at 7T. Magn Reson Med Sci 2015; 14:35–41.
8. Watanabe H. Investigation of the asymmetric distributions of RF transmission and reception fields at high static field. Magn Reson Med Sci 2012; 11:129–135.
9. Bianciardi M, Fukunaga M, van Gelderen P, et al. Sources of functional magnetic resonance imaging signal fluctuations in the human brain at rest: a 7 T study. Magn Reson Imaging 2009; 27:1019–1029.
10. Harada T, Kudo K, Uwano I, et al. Breath-holding during the calibration scan improves the reproducibility of parallel transmission at 7T for human brain. Magn Reson Med Sci 2017; 16:23–31.

11. Kameda H, Kudo K, Matsuda T, et al. Improvement of the repeatability of parallel transmission at 7T using interleaved acquisition in the calibration scan. J Magn Reson Imaging 2018; 48:94–101.

12. Roemer PB, Edelstein WA, Hayes CE, et al. The NMR phased array. Magn Reson Med 1990; 16:192–225.

13. Fujita H. New horizons in MR technology: RF coil designs and trends. Magn Reson Med Sci 2007; 6:29–42.

14. McGee KP, Stormont RS, Lindsay SA, et al. Characterization and evaluation of a flexible MRI receive coil array for radiation therapy MR treatment planning using highly decoupled RF circuits. Phys Med Biol 2018; 63:08NT02.

15. Ishii S, Hara T, Nanbu T, et al. Optimized workflow and imaging protocols for whole-body oncologic PET/MRI. Jpn J Radiol 2016; 34:754–762.

16. Wiesinger F, Bylund M, Yang J, et al. Zero TE-based pseudo-CT image conversion in the head and its application in PET/MR attenuation correction and MR-guided radiation therapy planning. Magn Reson Med 2018; 80:1440–1451.

17. Gong K, Yang J, Kim K, et al. Attenuation correction for brain PET imaging using deep neural network based on Dixon and ZTE MR images. Phys Med Biol 2018; 63:125011.

18. Zeng F, Nogami M, Ueno YR, et al. Diagnostic performance of zero-TE lung MR imaging in FDG PET/MRI for pulmonary malignancies. Eur Radiol 2020; 30:4995–5003.

19. Okazawa H, Higashino Y, Tsujikawa T, et al. Noninvasive method for measurement of cerebral blood flow using O-15 water PET/MRI with ASL correlation. Eur J Radiol 2018; 105:102–109.

20. Akram MSH, Obata T, Yamaya T. Microstrip transmission line RF coil for a PET/MRI insert. Magn Reson Med Sci 2020; 19:147–153.

21. Ichikawa S, Motosugi U, Omori M, et al. MR-guided focused ultrasound for uterine fibroids: a preliminary study of relationship between the treatment outcomes and factors of MR images including elastography. Magn Reson Med Sci 2019; 18:82–87.

22. Elias WJ, Lipsman N, Ondo WG, et al. A randomized trial of focused ultrasound thalamotomy for essential tremor. N Engl J Med 2016; 375:730–739.

23. Kuroda K. MR techniques for guiding high-intensity focused ultrasound (HIFU) treatments. J Magn Reson Imaging 2018; 47:316–331.

24. Pruessmann KP, Weiger M, Scheidegger MB, et al. SENSE: sensitivity encoding for fast MRI. Magn Reson Med 1999; 42:952–962.

25. Sodickson DK, Manning WJ. Simultaneous acquisition of spatial harmonics (SMASH): fast imaging with radiofrequency coil arrays. Magn Reson Med 1997; 38:591–603.

26. Griswold MA, Jakob PM, Heidemann RM, et al. Generalized autocalibrating partially parallel acquisitions (GRAPPA). Magn Reson Med 2002; 47:1202–1210.

27. Takizawa M, Goto T, Mochizuki H, et al. Cardiac cine parallel imaging on a 0.7T open system. Magn Reson Med Sci 2004; 3:45–49.

28. Takizawa M, Shimoda T, Nonaka M, et al. Parallel imaging of head with a dedicated multi-coil on a 0.4T open MRI. Magn Reson Med Sci 2005; 4:95–101.

29. Mori H, Aoki S, Masumoto T, et al. Two-dimensional magnetic resonance digital subtraction angiography using array spatial sensitivity encoding techniques in the assessment of intracranial hemodynamics. Radiat Med 2002; 20:223–229.

30. Kimura T, Kusahara H. Real-based Polarity-preserving Asymmetric Fourier Imaging (RepAFI). Magn Reson Med Sci 2017; 16:159–168.

31. Kimura T, Shigeta T. Magnitude-based asymmetric fourier imaging (MagAFI). Magn Reson Med Sci 2016; 15:94–104.

32. Lustig M, Donoho D, Pauly JM. Sparse MRI: the application of compressed sensing for rapid MR imaging. Magn Reson Med 2007; 58:1182–1195.

33. Ito S, Arai H, Yamada Y. Compressed sensing in magnetic resonance imaging using the multi-step Fresnel domain band split transformation. Magn Reson Med Sci 2012; 11:243–252.

34. Kromrey ML, Funayama S, Tamada D, et al. Clinical evaluation of respiratory-triggered 3D MRCP with navigator echoes compared to breath-hold acquisition using compressed sensing and/or parallel imaging. Magn Reson Med Sci 2020; 19:318–323.

35. Yoon JK, Kim MJ, Lee S. Compressed sensing and parallel imaging for double hepatic arterial phase acquisition in gadoxetate-enhanced dynamic liver magnetic resonance imaging. Invest Radiol 2019; 54:374–382.

36. Takeshima H, Saitoh K, Nitta S, et al. Estimation of spatio-temporal sensitivity using band-limited signals with no additional acquisitions for k-t parallel imaging. Magn Reson Med Sci 2019; 18:19–28.

37. Okuda S, Yamada Y, Tanimoto A, et al. Three-dimensional cardiac cine imaging using the kat ARC acceleration: Initial experience in clinical adult patients at 3T. Magn Reson Imaging 2015; 33:911–917.

38. Sekine T, Amano Y, Takagi R, et al. Feasibility of 4D flow MR imaging of the brain with either Cartesian y-z radial sampling or k-t SENSE: comparison with 4D Flow MR imaging using SENSE. Magn Reson Med Sci 2014; 13:15–24.

39. Glover GH. Phase-offset multiplanar (POMP) volume imaging: a new technique. J Magn Reson Imaging 1991; 1:457–461.

40. Setsompop K, Gagoski BA, Polimeni JR, et al. Blipped-controlled aliasing in parallel imaging for simultaneous multislice echo planar imaging with reduced g-factor penalty. Magn Reson Med 2012; 67:1210–1224.

41. Iwadate Y, Brau AC, Vasanawala SS, et al. Enhancement of respiratory navigator-gated three-dimensional spoiled gradient-recalled echo sequence with variable flip angle scheme. Magn Reson Med 2014; 72:172–177.

42. Takizawa M, Ito T, Itagaki H, et al. Modified echo peak correction for radial acquisition regime (RADAR). Magn Reson Med Sci 2009; 8:149–158.

43. Pipe JG. Motion correction with PROPELLER MRI: application to head motion and free-breathing cardiac imaging. Magn Reson Med 1999; 42:963–969.

44. Chandarana H, Feng L, Block TK, et al. Free-breathing contrast-enhanced multiphase MRI of the liver using a combination of compressed sensing, parallel imaging, and golden-angle radial sampling. Invest Radiol 2013; 48:10–16.

45. Ichikawa S, Motosugi U, Kromrey ML, et al. Utility of stack-of-stars acquisition for hepatobiliary phase imaging without breath-holding. Magn Reson Med Sci 2020; 19:99–107.

46. Nakamura Y, Higaki T, Nishihara T, et al. Pseudo-random trajectory scanning suppresses motion artifacts on gadoxetic acid-enhanced hepatobiliary-phase magnetic resonance images. Magn Reson Med Sci 2020; 19:21–28.

47. White N, Roddey C, Shankaranarayanan A, et al. PROMO: real-time prospective motion correction in MRI using image-based tracking. Magn Reson Med 2010; 63:91–105.

48. Watanabe K, Kakeda S, Igata N, et al. Utility of real-time prospective motion correction (PROMO) on 3D T1-weighted imaging in automated brain structure measurements. Sci Rep 2016; 6:38366.

49. Kyme AZ, Aksoy M, Henry DL, et al. Marker-free optical stereo motion tracking for in-bore MRI and PET-MRI application. Med Phys 2020; 47:3321–3331.

50. Tamada D, Kromrey ML, Ichikawa S, et al. Motion artifact reduction using a convolutional neural network for dynamic contrast enhanced MR imaging of the liver. Magn Reson Med Sci 2020; 19:64–76.

51. Kidoh M, Shinoda K, Kitajima M, et al. Deep learning based noise reduction for brain MR imaging: tests on phantoms and healthy volunteers. Magn Reson Med Sci 2020; 19:195–206.

52. Nakajima S, Fushimi Y, Yokota Y, et al. Application of deep learning reconstruction to compressed-sensing thin-slice fat-suppressed T2-weighted imaging of the orbit. Proceedings of the 28th Annual Meeting of ISMRM, On-line, 2020; 2024.

53. Kiryu S, Sugano Y, Ohta T, et al. Deep learning-based adaptive noise reduction for improving image quality of 1.5T MR images. Proceedings of the 28th Annual Meeting of ISMRM, On-line, 2020; 3624.

54. van Beek EJR, Kuhl C, Anzai Y, et al. Value of MRI in medicine: more than just another test?. J Magn Reson Imaging 2019; 49:e14-e25.

55. Yokoyama K, Ishimura R, Kariyasu T, et al. Clinical application of an automatic slice-alignment method for cardiac MR imaging. Magn Reson Med Sci 2014; 13:293–298.

56. Blansit K, Retson T, Masutani E, et al. Deep learning-based prescription of cardiac MRI planes. Radiol Artif Intell 2019; 1: e180069.

57. Sreekumari A, Shanbhag D, Yeo D, et al. A deep learning-based approach to reduce rescan and recall rates in clinical MRI examinations. AJNR Am J Neuroradiol 2019; 40:217–223.

58. Goto T, Kabasawa H. Automated scan prescription for MR imaging of deformed and normal livers. Magn Reson Med Sci 2013; 12:11–20.

59. Goto T, Kabasawa H. Robust automated bolus tracker positioning for MRI liver scans. Magn Reson Imaging 2015; 33:63–71.

60. Miyazaki M, Sugiura S, Tateishi F, et al. Non-contrast-enhanced MR angiography using 3D ECG-synchronized half-Fourier fast spin echo. J Magn Reson Imaging 2000; 12:776–783.

61. Miyazaki M, Akahane M. Non-contrast enhanced MR angiography: established techniques. J Magn Reson Imaging 2012; 35:1–19.

62. Takei N, Miyoshi M, Kabasawa H. Noncontrast MR angiography for supraaortic arteries using inflow enhanced inversion recovery fast spin echo imaging. J Magn Reson Imaging 2012; 35:957–962.

63. Shibukawa S, Konta N, Niwa T, et al. Non-enhanced and Non-gated MR angiography for robust visualization of peripheral arteries using enhanced Acceleration-selective Arterial Spin Labeling (eAccASL). Magn Reson Med Sci 2021; 20:312–319.

64. Suzuki Y, Fujima N, van Osch MJP. Intracranial 3D and 4D MR angiography using arterial spin labeling: technical considerations. Magn Reson Med Sci 2020; 19:294–309.

65. Irie R, Suzuki M, Yamamoto M, et al. Assessing blood flow in an intracranial stent: a feasibility study of MR angiography using a silent scan after stent-assisted coil embolization for anterior circulation aneurysms. AJNR Am J Neuroradiol 2015; 36:967–970.

66. Iima M. Perfusion-driven Intravoxel Incoherent Motion (IVIM) MRI in oncology: applications, challenges, and future trends. Magn Reson Med Sci 2021; 20:125–138.

67. Yamada K, Sakai K, Akazawa K, et al. MR tractography: a review of its clinical applications. Magn Reson Med Sci 2009; 8:165–174.

68. Hori M, Fukunaga I, Masutani Y, et al. Visualizing non-Gaussian diffusion: clinical application of q-space imaging and diffusional kurtosis imaging of the brain and spine. Magn Reson Med Sci 2012; 11:221–233.

69. Maekawa T, Kamiya K, Murata K, et al. Time-dependent diffusion in transient splenial lesion: comparison between oscillating-gradient spin-echo measurements and Monte-Carlo simulation. Magn Reson Med Sci 2021; 20:227–230.

70. Kabasawa H, Masutani Y, Aoki S, et al. 3T PROPELLER diffusion tensor fiber tractography: a feasibility study for cranial nerve fiber tracking. Radiat Med 2007; 25:462–466.

71. Mori N, Mugikura S, Miyashita M, et al. Turbo spin-echo diffusion-weighted imaging compared with single-shot echo-planar diffusion-weighted imaging: image quality and diagnostic performance when differentiating between ductal carcinoma in situ and invasive ductal carcinoma. Magn Reson Med Sci 2021; 1:60–68.

72. Kishimoto AO, Kataoka M, Iima M, et al. Evaluation of malignant breast lesions using high-resolution readout-segmented diffusion-weighted echo-planar imaging: comparison with pathology. Magn Reson Med Sci 2021; 20:204–215.

73. Kamimura K, Nakajo M, Yoneyama T, et al. Amide proton transfer imaging of tumors: theory, clinical applications, pitfalls, and future directions. Jpn J Radiol 2019; 37:109–116.

74. Kanazawa Y, Fushimi Y, Sakashita N, et al. B1 power optimization for chemical exchange saturation transfer imaging: a phantom study using egg white for amide proton transfer imaging applications in the human brain. Magn Reson Med Sci 2018; 17:86–94.

75. Ichikawa S, Motosugi U, Ichikawa T, et al. Magnetic resonance elastography for staging liver fibrosis in chronic hepatitis C. Magn Reson Med Sci 2012; 11:291–297.

76. Yoshimitsu K, Shinagawa Y, Mitsufuji T, et al. Preliminary comparison of multi-scale and multi-model direct inversion algorithms for 3T MR elastography. Magn Reson Med Sci 2017; 16:73–77.

77. Sato R, Shirai T, Taniguchi Y, et al. Quantitative susceptibility mapping using the multiple dipole-inversion combination with k-space segmentation method. Magn Reson Med Sci 2017; 16:340–350.

78. Kan H, Arai N, Takizawa M, et al. Improvement of signal inhomogeneity induced by radio-frequency transmit-related phase error for single-step quantitative susceptibility mapping reconstruction. Magn Reson Med Sci 2019; 18:276–285.

79. Ikebe Y, Ishimaru H, Imai H, et al. Quantitative susceptibility mapping for carotid atherosclerotic plaques: a pilot study. Magn Reson Med Sci 2020; 19:135–140.

80. Fujita S, Buonincontri G, Cencini M, et al. Repeatability and reproducibility of human brain morphometry using three-dimensional magnetic resonance fingerprinting. Hum Brain Mapp 2021; 42:275–285.

81. Fujita S, Hagiwara A, Takei N, et al. Accelerated isotropic multi-parametric imaging by high spatial resolution 3D-QALAS with compressed sensing: a phantom, volunteer, and patient study. Invest Radiol 2021; 56:292–300.

82. Xue H, Inati S, Sørensen TS, Hansen MS, et al. Distributed MRI reconstruction using Gadgetron-based cloud computing. Magn Reson Med 2015; 73:1015–1025.

83. Chelu RG, Wanambiro KW, Hsiao A, et al. Cloud-processed 4D CMR flow imaging for pulmonary flow quantification. Eur J Radiol 2016; 85:1849–1856.

84. Dietrich BE, Brunner DO, Wilm BJ, et al. A field camera for MR sequence monitoring and system analysis. Magn Reson Med 2016; 75:1831–1840.

85. Kodama N, Setoi A, Kose K. Spiral MRI on a 9.4T vertical-bore superconducting magnet using unshielded and self-shielded gradient coils. Magn Reson Med Sci 2018; 17:174–183.

86. Matsuo-Hagiyama C, Watanabe Y, Tanaka H, et al. Comparison of silent and conventional MR imaging for the evaluation of myelination in children. Magn Reson Med Sci 2017; 16:209–216.

87. Iwadate Y, Nozaki A, Nunokawa Y, et al. Comparison of silent navigator waveform generation methods. Magn Reson Med Sci 2020; 19:154–158.